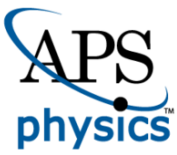

Memory Formation in Jammed Hard Spheres

Patrick Charbonneau and Peter K. Morse

Phys. Rev. Lett. **126**, 088001 — Published 22 February 2021

DOI: 10.1103/PhysRevLett.126.088001

Memory Formation in Jammed Hard Spheres

Patrick Charbonneau[1, 2] and Peter K. Morse[1, *]

[1] *Department of Chemistry, Duke University, Durham, North Carolina 27708*
[2] *Department of Physics, Duke University, Durham, North Carolina 27708*

(Dated: December 18, 2020)

Liquids equilibrated below an onset condition share similar inherent states, while those above that onset have inherent states that markedly differ. Although this type of materials memory was first reported in simulations over 20 years ago, its physical origin remains controversial. Its absence from mean-field descriptions, in particular, has long cast doubt on its thermodynamic relevance. Motivated by a recent theoretical proposal, we reassess the onset phenomenology in simulations using a fast hard sphere jamming algorithm and find it to be both thermodynamically and dimensionally robust. Remarkably, we also uncover a second type of memory associated with a Gardner-like regime of the jamming algorithm.

The state of a material is nominally the product of its history, echoing both states and processes previously encountered. Yet equilibrium states are memoryless. Only certain non-equilibrium processes allow information to be stored, retained, and summoned back. Given the rich out-of-equilibrium physics of glass formers, these materials exhibit a rich variety of memory types, and thus broadly inform our understanding of the phenomenon. Spin glass models, in particular, form the theoretical basis for both machine and biological learning [1–3]. Their structural counteparts [4] form an even richer array of memory types via out-of-equilibrium processes as varied as shearing [5–7], heating cycles [8], and aging [9].

Inherent state memory, which relates an equilibrium state to its nearest energy minima or jammed configuration through a fast out-of-equilibrium quench [8, 10–12], is one of the simplest memory types in glasses. Which macroscopic properties of the original equilibrium state can an inherent structure recall? In *pure* p-spin models, which commonly inform the mean-field description of glasses [13], the answer is straightforward. Initial systems taken above the dynamical (or mode-coupling) transition temperature, T_d, are quenched to inherent states indistinguishable from one another [14]. In other words, no information about the original liquid persits, other than that it was a liquid. This memorylessness has long been argued to be a general feature of glass formers, but numerical simulations of (Kob-Andersen binary) Lennard-Jones liquids [15–18], model polymers [19], and soft spheres [20–23] do not concur. In these systems, all states prepared above an onset $T_\mathrm{on} > T_\mathrm{d}$ share a same inherent state energy, but inherent state energies of liquids prepared below T_on differ. The resulting amorphous solid thus seemingly encodes some features of the original liquid.

Attempts to explain away this discrepancy abound. Finite-size [24, 25] or finite-dimensional corrections [25, 26] have been invoked, measurement protocols have been questioned [20, 23], as has the validity of the analogy between spins and particles [25]. The solution of the glass problem in the high-dimensional, $d \to \infty$ limit [4], however, has revealed that the mean-field analogy between spin and structural glasses is quite strong, and some features of the glass phenomenology are remarkably robust to dimensional changes [13]. A novel proposal for resolving this discrepancy recently emerged from the work Folena et al. [27, 28], who realized that *mixed* p-spin models generically present an onset, and hence that *pure* p-spin models might be exceptional rather than typical (see also [29]).

This advance, however, does not address many of the remaining concerns, including algorithmic and finite-size considerations. In this letter, we use advanced computer simulations to eliminate these hypotheses and strongly evince the existence of a distinct landscape onset in liquids, and therefore fully resolve the crisis. We further uncover that the preparation algorithm itself bears signatures of an out-of-equilibrium transition, which strongly resembles the onset of a Gardner phase. We assess the properties of this transition, its relation to the jamming algorithm, and how it defines a memory that distinguishes between all initial liquid conditions, even before the onset is reached.

Model and Simulation Method— We consider the inherent states of hard sphere glass formers obtained by rapidly compressing (crunching), an equilibrated liquid of N particles at volume fraction ϕ_eq to its nearest jamming point [30]. Existing crunching algorithms either violate the hard sphere constraint [31–33], allow for significant equilibration [23, 34], or scale poorly with system size [35–38]. In order to avoid these pitfalls, we modify a recent algorithm by Arceri and Corwin [39] and propose the iterative scheme depicted schematically in Fig. 1a. Using the minimum scaled gap, $h = \min_{ij}(h_{ij}) = \min_{ij}[d_{ij}/(r_i + r_j)]$ between particles i and j of radii r_i and r_j a distance d_{ij} apart as reference, the nth step involves first an *inflation*, and then a *repulsion* substep. The former entails expanding particles uniformly, thus creating a new minimum gap, $h'_\mathrm{n} = \theta h_\mathrm{n}$, and the latter uses the FIRE algorithm [40] to minimize the effective thermal potential for hard spheres near jamming [41, 42], until $h_{\mathrm{n}+1} = h_\mathrm{n}$ [30]. The expansion factor, $\theta < 1$, ensures that the hard sphere constraint is never

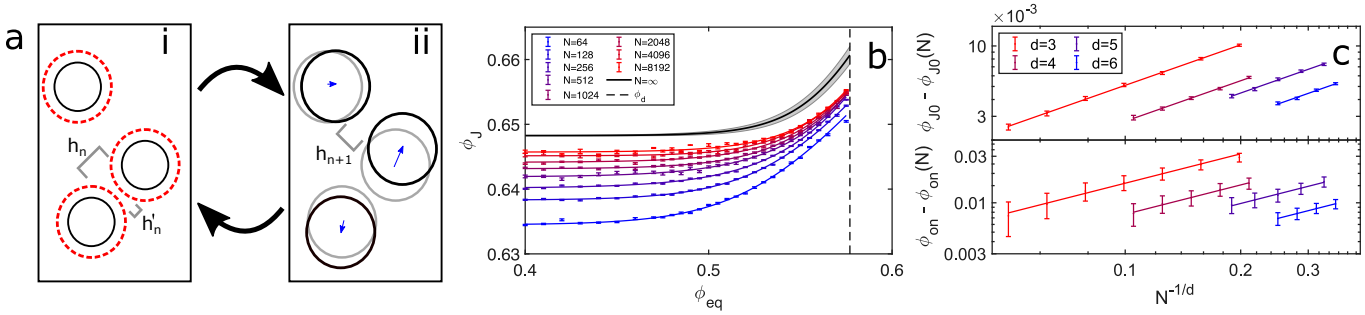

Figure 1. **a)** Schematic of the two-substep iterative jamming algorithm. **(i)** *Inflation*: particles (black disks) separated by minimum gap h_n expand uniformly (red disks) until h'_n. **(ii)** *Repulsion*: an effective free energy is minimized until the minimum gap reaches $h_{n+1} = h_n$. The cycle is repeated until density converges at jamming. **b)** The onset is clearly visible in $d = 3$ for all system sizes considered. Lines are fits to the phenomenological crossover form, Eq. (2). The thermodynamic $N \to \infty$ limit of the fit parameters (black line) shows that the onset appears well before the dynamical (mode-coupling) crossover (dashed black line). **c)** Finite-size scaling of the jamming transition ϕ_{J0} below the onset (top), and the finite-size scaling of the onset (below), where lines are fits to Eq. (1), and curves are offset for visual clarity.

violated. Although the minimal scaled gap stays constant from one step to the next, interparticle distances steadily decrease, and hence the algorithm converges at jamming. Interestingly, a marked algorithmic slowdown of the FIRE minimization arises well before jamming is reached. We thus cap the number of steps of this minimization to a small multiple of the degrees of freedom, $n_{\rm FIRE} = \tau N d$, to prevent a full minimization–and thus unwanted thermalization–as the crunching proceeds. The parameters θ and τ are optimized to achieve the lowest jamming density while reliably rigidifying the structure, thus ensuring that equilibration is maximally suppressed. We set $\theta = 0.9$ and $\tau = 2$ which are near optimal for $d = 3$ and appear to depend only weakly on dimension [30]. As a result, a low-density fluid crunched this way best approximates the maximally random jammed state [43], and does so fairly efficiently [30].

Onset Memory— The first quantity of interest is the density of jammed states $\phi_{J0}(N)$, obtained from low-density liquids, and its scaling with system size N upon approaching the thermodynamic $N \to \infty$ limit. Because of the critical nature of jamming, we expect

$$\phi_{J0} - \phi_{J0}(N) \sim N^{-1/\nu d} \qquad (1)$$

with correlation length exponent ν. Soft spheres studies have found $\nu \approx 0.7$ [20, 31, 45], which is inconsistent with $\nu \approx 1$ obtained from direct measurements of the correlation length at jamming [46]. We here robustly find $\nu \approx 1$ in all d, with $\nu = 1.01 \pm 0.04$, 0.99 ± 0.06, 1.01 ± 0.10, and 1.0 ± 0.3 in $d = 3$, 4, 5, and 6 respectively, thus resolving the discrepancy. Although different exponents can in principle be attributed to model and algorithmic differences [46], the scaling difference between soft and hard spheres might also originate from the fact that minimization of the former, unlike crunching of the latter, allows for weak barriers to be crossed. In support of this hypothesis, we note that our thermodynamic extrapolations for

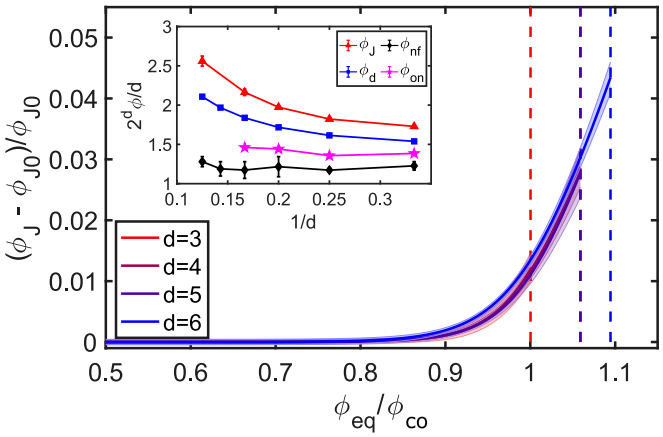

Figure 2. Infinite-system size onset curves for different dimensions can be collapsed, suggesting that the inherent structure onset exists in both the thermodynamic and the infinite-dimensional limits. Shaded regions give the standard error of Eq. (2) with 95% confidence intervals on parameters, and dashed lines denote ϕ_d from Ref. [44]. The steady increase of ϕ_d with dimension on this scale shows that $\phi_{co} < \phi_d$. The collapse further supports the identification $\phi_{on} \sim 0.9\phi_{co}$. **(Inset)** Scaling of ϕ_{J0} and ϕ_{on} with d, compared with those for the avoided dynamical transition, ϕ_d, and the onset of non-Fickian diffusion, ϕ_{nf}, from Ref. [44] reveals that both ϕ_{nf} and ϕ_{on} exhibit a trivial mean-field-like dimensional scaling down to physical dimensions, unlike ϕ_d and ϕ_{J0}.

ϕ_{J0} are close to but systematically smaller than those for soft spheres for all dimensions considered [30], including the careful estimate of Ref. 45. In addition, the lack of dimensional dependence of this particular critical exponent for a specific model and algorithm gives further credence to $d_u = 2$ being the lower critical dimension for jamming [47–49].

Figure 1c shows a clear dependence of the inherent state density on the original equilibrium liquid condition,

such that for $\phi_{\rm eq} \lesssim \phi_{\rm on}$, $\phi_{\rm J}$ is constant, and for $\phi_{\rm eq} \gtrsim \phi_{\rm on}$, $\phi_{\rm J}$ increases with $\phi_{\rm eq}$. The change from one regime to the other, however, does not sharpen as system size increases, and thus remains a crossover in the thermodynamic limit. To quantify this feature, we use the empirical softmax form [50]

$$\phi_{\rm J}(\phi_{\rm eq}) = \phi_{\rm J0} + ab\ln(1 + e^{(\phi_{\rm eq}-\phi_{\rm co})/b}), \qquad (2)$$

where $\phi_{\rm co}(N)$ marks the crossover point between the low density and high density linear regimes, $a = \frac{d\phi_{\rm J}}{d\phi_{\rm eq}}$ for $\phi_{\rm eq} \gg \phi_{\rm co}$, and $b(N)$ characterizes the width of the crossover region. This form nicely recapitulates our observations, but we note that $\phi_{\rm co}$ occurs well above the point at which $\phi_{\rm J}$ deviates from $\phi_{\rm J0}$, which traditionally defines the onset. Without loss of generality, we thus define $\phi_{\rm on} = 0.9\phi_{\rm co}$. The result scales as $\phi_{\rm on} \sim N^{-1/d}$ (Figure 1b). Because of the limited density range between $\phi_{\rm co}$ and $\phi_{\rm d}$, around which standard computations become particularly onerous for monodisperse systems, the fitting parameters a and b, cannot be independently determined at fixed N. Imposing that a single a should fit all N, however, suffices to obtain a robust extrapolation of Eq. (2) to the thermodynamic limit [30].

In order to compare the dimensional trend quantitatively, we consider the fractional deviation from $\phi_{\rm J0}$ with the normalized density growth $\phi_{\rm eq}/\phi_{\rm co}$. The thermodynamic onset results then collapse onto a master curve (Fig. 2), strongly suggesting that the onset persists as a crossover as $d \to \infty$. This scaling also shows that $\phi_{\rm co}$ and thus $\phi_{\rm on}$ are numerically distinct from the (avoided) dynamical transition $\phi_{\rm d}$ as indicated by the steady increase of $\phi_{\rm d}$ on this scale. Hence, independently of the proposed scaling, our results validate earlier numerical studies and are in sharp contrast with those of Ref. [14] for pure p-spin models. The inset of Fig. 2 suggests that upon considering the mean-field, $d \to \infty$, limit the onset remains roughly constant, while the (avoided) dynamical transition shifts markedly as d increases. Interestingly, this same qualitative behavior has been observed for another onset, that of non-Fickian diffusion, $\phi_{\rm nf}$ [44].

These various results also inform us about the role played by liquid structure. While the (avoided) dynamical transition is strongly affected by that structure [44, 51], the onset is not. As d increases, structure markedly simplifies [52, 53], yet the onset persists. Local structure therefore at most modulates the phenomenon [22]. This distinction suggests that separate underlying (landscape) mechanisms likely control these different features. Note also that although it is not immediately apparent why $\phi_{\rm on}$ and $\phi_{\rm nf}$ should scale similarly, the robustness of our results suggests that a complete out-of-equilibrium dynamical theory should account for their (near) coincidence.

Algorithmic Memory— Surprisingly, a second form of memory develops before jamming is reached. As a liquid is initially crunched, interparticle gaps first grow more regular, such that $\langle h\rangle/h_{\rm min} \sim 1$ (Figure 3a). Because of the disordered, and thus frustrated, nature of the jammed state, however, the repulsion sub-step becomes increasingly computationally arduous, as illustrated by the rapid growth in the number of minimization loops necessary to achieve $h_{\rm n+1} = h_{\rm n}$ (Fig. 3b). Gap regularization then also goes into reverse. Remarkably, the two phenomena coincide at some $\phi_{\rm G}$. This putative algorithmic onset can be further characterized by considering the outcome of perturbing a state along the jamming algorithm. Taking exact replicas at $\phi_{\rm break}$ and applying a single Metropolis Monte Carlo sweep before crunching anew gives rise to force contacts at jamming, c_i, that can vary.

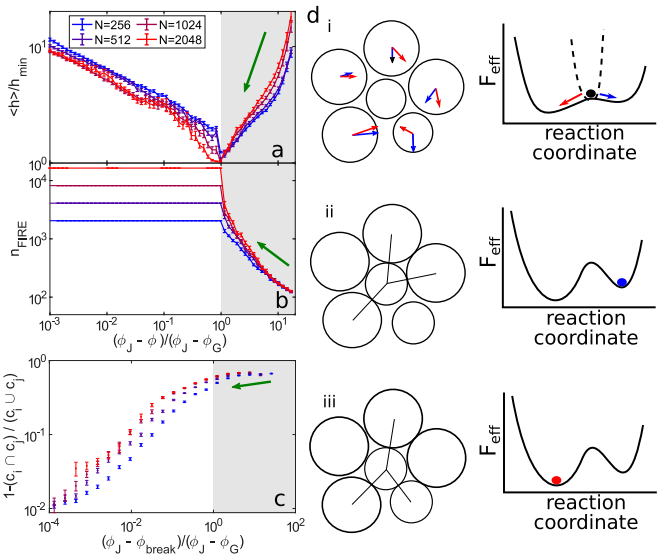

Figure 3. The onset of the algorithmic slowdown at $\phi_{\rm G}$ is simultaneously characterized by three observables, which robustly identify a change in the crunching process. The results shown here for $d = 4$ with $\phi_{\rm eq} = 0.2$ are typical of other d and $\phi_{\rm eq}$.) **a)** At $\phi_{\rm G}$, the distribution of gaps narrows significantly, such that the minimum gap most closely approaches the average gap. **b)** The number of minimization loops necessary to complete the repulsion substep of the jamming algorithm grows precipitously, and is manually cut off at $\tau = 2$. **c)** The correlation between contact networks, c_i, for an unperturbed system at jamming and, c_j, for a replica perturbed at $\phi_{\rm break}$ shows that systems perturbed before $\phi_{\rm G}$ (gray zone) end up with markedly different contact networks compared to systems perturbed beyond $\phi_{\rm G}$ (white zone). Increasing system size makes the effect more prominent and shifts the process to higher densities but nonetheless remain distinct from $\phi_{\rm J}$ [30]. **d)** Taken together, these observation suggest that saddles start to dominate the landscape of the crunch algorithm around $\phi_{\rm G}$, thus resulting in sluggish dynamics and a large contact network response to small perturbations in particle positions. In other words, a slightly perturbed system (i) jams as (iii), whereas the original system jams as (ii). This series of observations for an out-of-equilibrium algorithm is reminiscent of the Gardner-like behavior of quasi-static state followings in ultrastable glasses [54].

Comparing these contact networks highlights structural differences. The quantity $1-(c_i \cap c_j)/(c_i \cup c_j)$, in particular, vanishes if the packings are identical and unity if they share no contacts. Figure 3c indicates that applying a perturbation before ϕ_G results in markedly different jammed states, whereas perturbations made after ϕ_G result in increasingly small deviations. The spread in jamming density also correspondingly narrows [30].

Taken together these observations suggest that saddles start to dominate the optimization landscape around ϕ_G, forcing the selection of a nearby sub-basin and thus of a contact network at jamming (Fig. 3d). A transition which sharpened with system size above ϕ_G would imply that all replicas perturbed after ϕ_G converge on the same contact network. That it does not suggests instead a rich, multi-layered landscape structure reminiscent of an equilibrium Gardner regime [13, 54–56], for which mean-field theory predicts a fractal hierarchy of sub-basins [56].

The evolution of ϕ_G upon increasing ϕ_{eq} is akin to that of ϕ_J (Fig. 4), but with an initial linear growth instead of a density-independent regime [30]. To estimate if both this linear scaling and ϕ_G persist with increasing system size and dimension, we fit the results to a modified form of the softmax potential

$$\phi_G(\phi_{eq}) = \phi_{G0} + \Gamma(\phi_{eq} - \phi_{co}) + (a-\Gamma) b \ln(1 + e^{(\phi_{eq}-\phi_{co})/b}), \quad (3)$$

where a, b, and ϕ_{co} are taken from fits to Eq. (3), and $\Gamma = \left.\frac{d\phi_G}{d\phi_{eq}}\right|_0$ is the slope of the linear regime. Figure 4 shows that Γ tends to a constant as $N \to \infty$, and that this constant increases as d increases [30]. Hence, although systems prepared at different $\phi_{eq}^{(1)} < \phi_{eq}^{(2)} < \phi_{on}$ both jam at a density ϕ_{J0}, $\phi_{eq}^{(1)}$ encounters a saddle-dominated regime at smaller densities than $\phi_{eq}^{(2)}$. In other words, while the jammed state may not recall the liquid density used to prepare it, its crunching certainly notices.

The identification of ϕ_G, its similarity to a Gardner transition, and its echo of the onset provide guidance for solving out-of-equilibrium dynamical theories [29, 57, 58]. Indeed, while quasi-equilibrium calculations find that a Gardner transition is a necessary step towards jamming for liquids equilibrated beyond φ_d [54, 59], our results suggest that an equivalent out-of-equilibrium phenomenon should be uncovered in a mean-field description. If true, this would resolve the paradoxical observation that jamming criticality is obtained in the experimentally relevant regime [31, 48, 60, 61], with $\phi \ll \phi_{on}$, even in absence of quasi-equilibrium Gardner physics.

Conclusion— By devising an efficient crunching algorithm that does not violate the hard-sphere condition, we have determined that inherent state memory persists in the thermodynamic and high-dimensional limits. Such memory thus ought to exist in mean-field descriptions. We have further identified a Gardner-like point in the strongly out-of-equilibrium behavior of our crunching algorithm. This quantity itself varies across ϕ_{eq}, and thus encodes a second type of memory of the original liquid, even at densities well below the inherent structure onset. Although the value of ϕ_G is likely strongly algorithm dependent, we expect all such procedures to encounter a comparable slowdown or instability. Revisiting such algorithms might be particularly instructive, and could offer insight into a broader class of problems, particularly within generalized learning algorithms, for which interest in Gardner physics has recently grown [62]. If the association between Gardner physics and strongly out-of-equilibrium jamming is confirmed, then experimental validations of the Gardner physics should then also be well within reach.

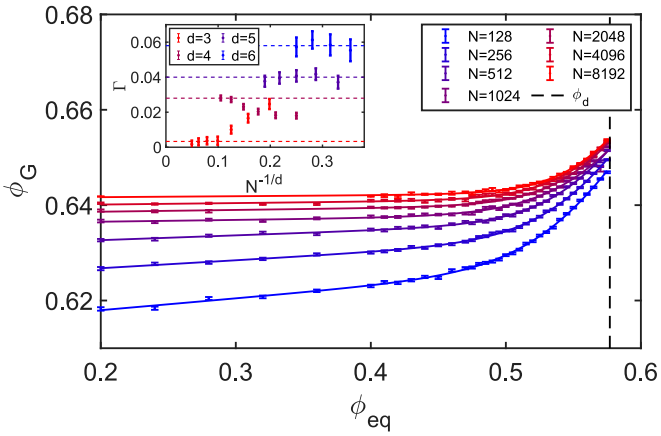

Figure 4. **a)** The algorithmic ϕ_G in $d = 3$, identified as in Fig. 3, shifts with system size. **(Inset)** The low-density slope of ϕ_G tends to a finite value as N increases in all dimensions (dashed lines). Because the density dependence of $\phi < \phi_{on}$ seemingly persists in the thermodynamic limit, memory of the initial state appears upon crunching.

We acknowledge many stimulating discussions with Ada Altieri, Francesco Arceri, Silvio Franz, Jorge Kurchan, Giorgio Parisi, and Francesco Zamponi. This work was supported by the Simons Foundation grant # 454937. Most simulations were performed at Duke Compute Cluster (DCC), for which the authors thank Tom Milledge's assistance. The authors also thank the Extreme Science and Engineering Discovery Environment (XSEDE), supported by National Science Foundation Grant No. ACI-1548562, for computer time. Data relevant to this work have been archived and can be accessed at the Duke Digital Repository `https://doi.org/10.7924/XXXXXXX`.

* Corresponding author.; peter.k.morse@gmail.com

[1] D. L. Stein, *Spin Glasses and Biology*, Series on Directions in Condensed Matter Physics, Vol. 6 (World Scientific, 1992).

[2] A. Choromanska, M. Henaff, M. Mathieu, G. B. Arous, and Y. LeCun, in *Journal of Machine Learning Research*, Vol. 38 (2015) pp. 192–204.

[3] M. Baity-Jesi, L. Sagun, M. Geiger, S. Spigler, G. B. Arous, C. Cammarota, Y. LeCun, M. Wyart, and G. Biroli, J. Stat. Mech. **2019**, 124013 (2019).

[4] G. Parisi, P. Urbani, and F. Zamponi, *Theory of Simple Glasses: Exact Solutions in Infinite Dimensions* (Cambridge University Press, 2020).

[5] J. D. Paulsen, N. C. Keim, and S. R. Nagel, Phys. Rev. Lett. **113**, 068301 (2014).

[6] D. R. Reid, N. Pashine, J. M. Wozniak, H. M. Jaeger, A. J. Liu, S. R. Nagel, and J. J. de Pablo, Proc. Natl. Acad. Sci. U.S.A. **115**, E1384 (2018).

[7] N. C. Keim, J. D. Paulsen, Z. Zeravcic, S. Sastry, and S. R. Nagel, Rev. Mod. Phys. **91**, 035002 (2019).

[8] P. Debenedetti and F. Stillinger, Nature **410**, 259 (2001).

[9] C. A. Angell, K. L. Ngai, G. B. McKenna, P. F. McMillan, and S. W. Martin, J. Appl. Phys. **88**, 3113 (2000).

[10] R. J. Speedy, J. Phys. Condens. Matter **10**, 4185 (1998).

[11] A. Heuer, J. Phys.-Condens. Mat. **20**, 373101 (2008).

[12] R. Mari, F. Krzakala, and J. Kurchan, Phys. Rev. Lett. **103**, 025701 (2009).

[13] P. Charbonneau, J. Kurchan, G. Parisi, P. Urbani, and F. Zamponi, Annu. Rev. Conden. Ma. P. **8**, 265 (2017).

[14] L. F. Cugliandolo and J. Kurchan, Phys. Rev. Lett. **71**, 173 (1993).

[15] S. Sastry, P. G. Debenedetti, and F. H. Stillinger, Nature **393**, 554 (1998).

[16] S. Sastry, Phys. Chem. Comm. **3**, 79 (2000).

[17] Y. Brumer and D. R. Reichman, Phys. Rev. E **69**, 041202 (2004).

[18] S. Sastry, J. Indian I. Sci. **86**, 731 (2013).

[19] S. Kamath, R. H. Colby, S. K. Kumar, and J. Baschnagel, J. Chem. Phys. **116**, 865 (2001).

[20] M. Ozawa, T. Kuroiwa, A. Ikeda, and K. Miyazaki, Phys. Rev. Lett. **109**, 205701 (2012).

[21] L. Berthier, D. Coslovich, A. Ninarello, and M. Ozawa, Phys. Rev. Lett. **116**, 238002 (2016).

[22] M. Ozawa, L. Berthier, and D. Coslovich, SciPost Physics **3**, 027 (2017).

[23] Y. Jin and H. Yoshino, arXiv:2003.10814 [cond-mat] (2020).

[24] A. Crisanti and F. Ritort, Europhys. Lett. **51**, 147 (2000).

[25] C. Dasgupta and O. T. Valls, J. Phys.-Condens. Mat. **12**, 6553 (2000).

[26] S. C. Glotzer, N. Jan, and P. H. Poole, J. Phys.-Condens. Mat. **12**, 6675 (2000).

[27] G. Folena, S. Franz, and F. Ricci-Tersenghi, Phys. Rev. X **10**, 031045 (2020).

[28] F. Zamponi, Journal Club for Condensed Matter Physics (2019), 10.36471/JCCM_June_2019_03.

[29] A. Altieri, G. Biroli, and C. Cammarota, J. Phys. A-Math. Theor. **53**, 375006 (2020).

[30] See Supplemental Material for details about the hard sphere model [63–65], the effective potential, optimizing the crunching algorithm and it's computational efficiency, the comparison to soft sphere jamming, the onset results in $d = 4 - 6$, and the finite-size scaling analysis of the jamming network under state following.

[31] C. S. O'Hern, L. E. Silbert, A. J. Liu, and S. R. Nagel, Phys. Rev. E **68**, 011306 (2003).

[32] S. S. Ashwin, J. Blawzdziewicz, C. S. O'Hern, and M. D. Shattuck, Phys. Rev. E **85**, 061307 (2012).

[33] P. K. Morse and E. I. Corwin, Phys. Rev. Lett. **112**, 115701 (2014).

[34] B. D. Lubachevsky and F. H. Stillinger, J. Stat. Phys. **60**, 561 (1990).

[35] E. Lerner, G. Düring, and M. Wyart, Comput. Phys. Commun. **184**, 628 (2013).

[36] C. Artiaco, P. Baldan, and G. Parisi, Phys. Rev. E **101**, 052605 (2020).

[37] R. D. H. Rojas, G. Parisi, and F. Ricci-Tersenghi, Soft Matter (2020).

[38] While significantly slower than their simple hard sphere counterparts, fast polymer crunching algorithms obeying the hard sphere limit exist [66, 67] and can be used to show the robustness of the onset in more complex fluids [19].

[39] F. Arceri and E. I. Corwin, Phys. Rev. Lett. **124**, 238002 (2020).

[40] E. Bitzek, P. Koskinen, F. Gähler, M. Moseler, and P. Gumbsch, Phys. Rev. Lett. **97**, 170201 (2006).

[41] C. Brito and M. Wyart, Europhys. Lett. **76**, 149 (2006).

[42] A. Altieri, S. Franz, and G. Parisi, J. Stat. Mech. **2016**, 093301 (2016).

[43] S. Torquato, T. M. Truskett, and P. G. Debenedetti, Phys. Rev. Lett. **84**, 2064 (2000).

[44] P. Charbonneau, Y. Jin, G. Parisi, and F. Zamponi, Proc. Natl. Acad. Sci. U.S.A. **111**, 15025 (2014).

[45] C. S. O'Hern, S. A. Langer, A. J. Liu, and S. R. Nagel, Phys. Rev. Lett. **88**, 075507 (2002).

[46] D. Vågberg, D. Valdez-Balderas, M. A. Moore, P. Olsson, and S. Teitel, Phys. Rev. E **83**, 030303 (2011).

[47] M. Wyart, Ann. Phys. Fr. **30**, 1 (2005).

[48] C. P. Goodrich, A. J. Liu, and S. R. Nagel, Phys. Rev. Lett. **109**, 095704 (2012).

[49] D. Hexner, P. Urbani, and F. Zamponi, Phys. Rev. Lett. **123**, 068003 (2019).

[50] C. Dugas, Y. Bengio, F. Bélisle, C. Nadeau, and R. Garcia, in *Advances in Neural Information Processing Systems 13* (MIT Press, 2001) pp. 472–478.

[51] M. Mangeat and F. Zamponi, Phys. Rev. E **93**, 012609 (2016).

[52] B. Charbonneau, P. Charbonneau, and G. Tarjus, Phys. Rev. Lett. **108**, 035701 (2012).

[53] B. Charbonneau, P. Charbonneau, and G. Tarjus, J. Chem. Phys. **138**, 12A515 (2013).

[54] L. Berthier, P. Charbonneau, Y. Jin, G. Parisi, B. Seoane, and F. Zamponi, Proc. Natl. Acad. Sci. U.S.A. **113**, 8397 (2016).

[55] P. Charbonneau, E. I. Corwin, L. Fu, G. Tsekenis, and M. van der Naald, Phys. Rev. E **99**, 020901 (2019).

[56] P. Charbonneau, J. Kurchan, G. Parisi, P. Urbani, and F. Zamponi, Nat. Commun. **5**, 3725 (2014).

[57] E. Agoritsas, G. Biroli, P. Urbani, and F. Zamponi, J. Phys. A-Math. Theor. **51**, 085002 (2018).

[58] E. Agoritsas, T. Maimbourg, and F. Zamponi, J. Phys. A-Math. Theor. **52**, 334001 (2019).

[59] L. Berthier, G. Biroli, P. Charbonneau, E. I. Corwin, S. Franz, and F. Zamponi, J. Chem. Phys. **151**, 010901 (2019).

[60] E. Lerner, G. Düring, and M. Wyart, Soft Matter **9**, 8252 (2013).

[61] P. Charbonneau, E. I. Corwin, G. Parisi, and F. Zamponi, Phys. Rev. Lett. **114**, 125504 (2015).

[62] A. Abbara, B. Aubin, F. Krzakala, and L. Zdeborová, in *Proceedings of Machine Learning Research*, Vol. 107

(2020) pp. 27–54.
[63] J. A. van Meel, B. Charbonneau, A. Fortini, and P. Charbonneau, Phys. Rev. E **80**, 061110 (2009).
[64] M. Skoge, A. Donev, F. H. Stillinger, and S. Torquato, Phys. Rev. E **74**, 041127 (2006).
[65] K. Zhang, W. W. Smith, M. Wang, Y. Liu, J. Schroers, M. D. Shattuck, and C. S. O'Hern, Phys. Rev. E **90**, 032311 (2014).
[66] N. C. Karayiannis and M. Laso, Phys. Rev. Lett. **100**, 050602 (2008).
[67] P. M. Ramos, N. C. Karayiannis, and M. Laso, J. Comput. Phys. **375**, 918 (2018).